Supplementary material: Performance evaluation of the Alphasense OPC-N3 and Plantower PMS5003 sensor in measuring dust events in the Salt Lake Valley, Utah

Section S1: Multilinear regression

A multilinear regression was performed with FEM-HW PM_{10} as the dependent variable and OPC-HW, and relative humidity (RH) as independent variables.

Without considering the effect of the RH:

	Intercept Coefficient ($\mu g/m^3$)	Intercept Standard Error ($\mu g/m^3$)	PM_{10} OPC-HW MLR Coefficient	PM_{10} OPC-HW Standard Error	R^2	Adjusted R^2	RMSE ($\mu g/m^3$)
PM_{10} FEM-HW	3.74	0.581	0.939	0.0148	0.865	0.865	12.0

Considering the RH:

	Intercept Coefficient ($\mu g/m^3$)	Intercept Standard Error ($\mu g/m^3$)	RH % MLR Coefficient	RH % Standard Error	PM_{10} OPC-HW MLR Coefficient	PM_{10} OPC-HW Standard Error	R^2	Adjusted R^2	RMSE ($\mu g/m^3$)
PM_{10} FEM-HW	9.65	1.11	-0.153	0.0247	0.928	0.0145	0.872	0.872	11.7

The inclusion of RH did not increase the correlation significantly. Therefore, the low-cost sensors measurements were not corrected for the relative humidity.

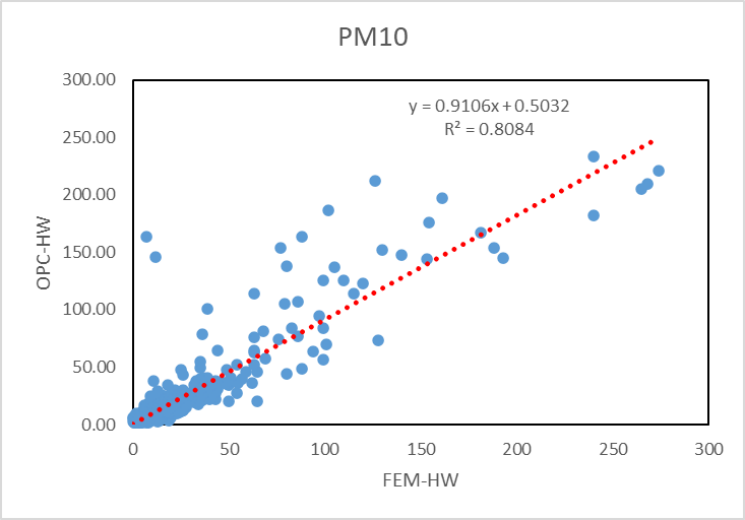

Fig S1: Correlation between OPC-N3 and FEM at HW for PM_{10}. The plot includes all the measurements including measurements with corresponding high relative humidity (>85%).

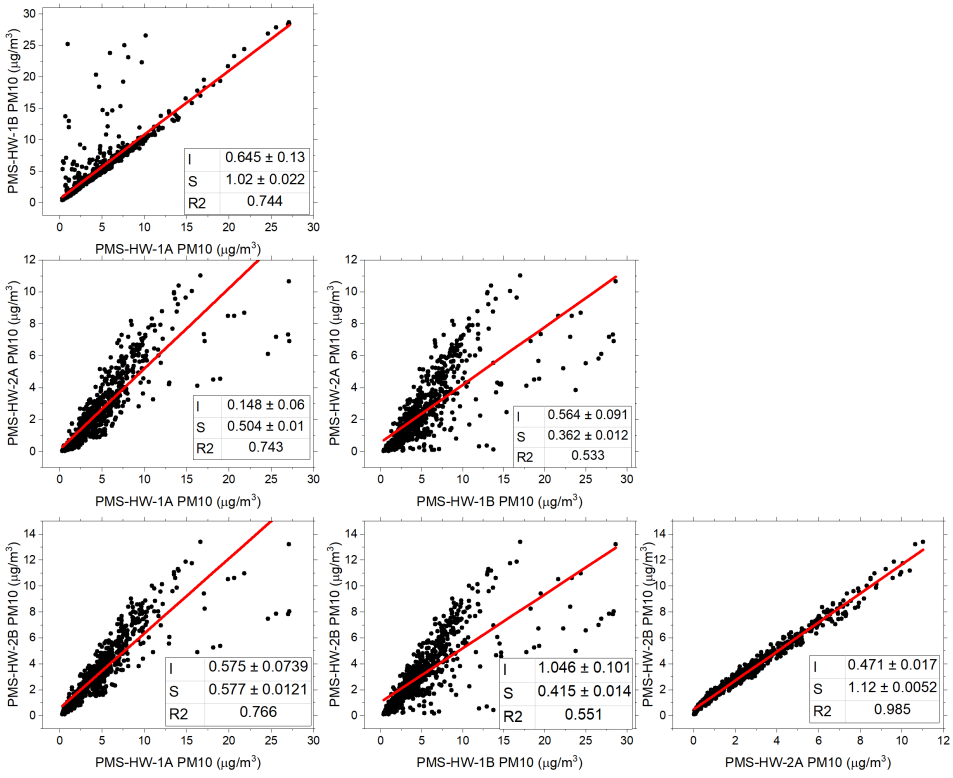

Figure S2: Inter-sensor correlation of PMS5003 sensors at HW site for PM_{10} concentrations. The plot includes measurements recorded between 04/1/2022 – 04/30/2022. I: intercept; S: slope.

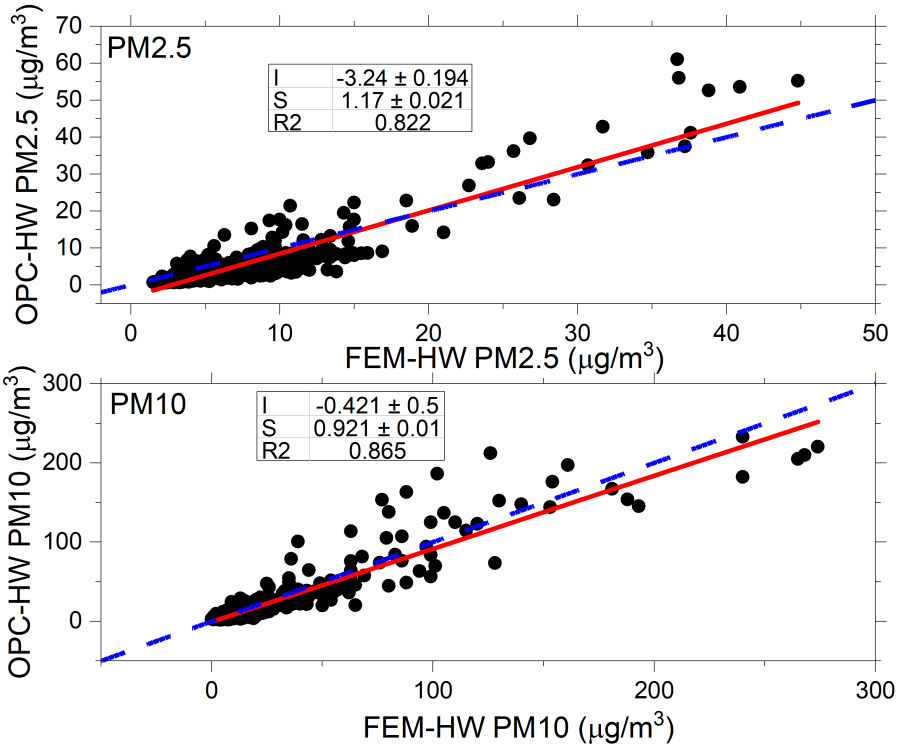

Figure S3: $PM_{2.5}$ and PM_{10} concentrations for OPC-HW and FEM-HW at HW site. The plot includes measurements recorded between 04/1/2022 – 04/30/2022. I: intercept; S: slope.

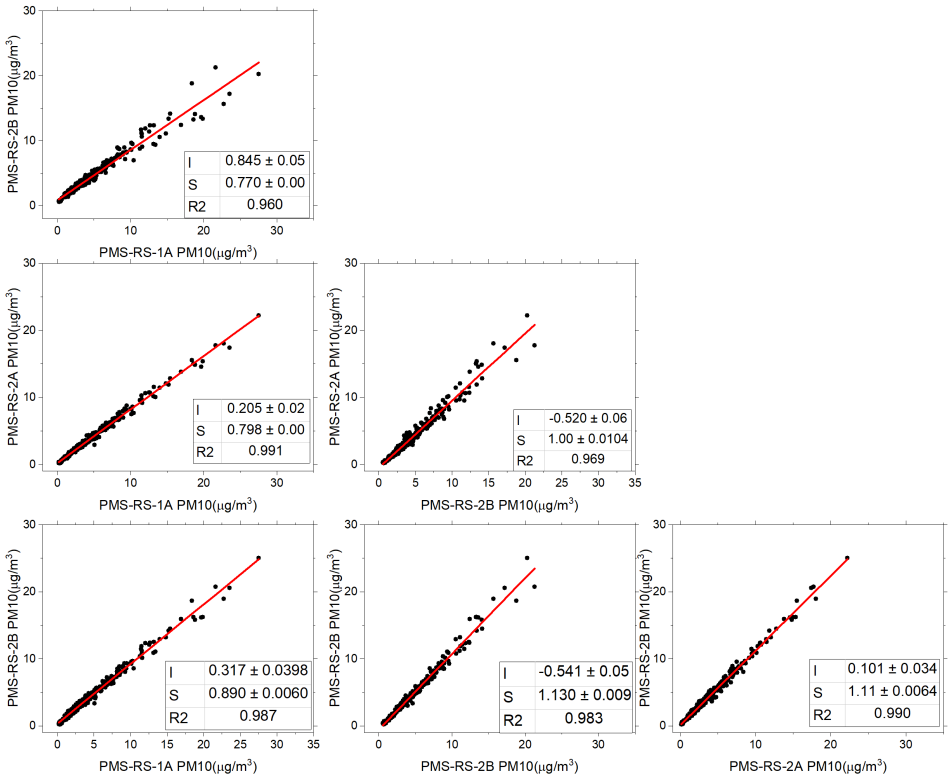

Figure S4: Inter-sensor correlation for the PMS5003 sensors at the RS site. The plot includes measurements recorded between 04/18/2022 – 04/30/2022. I: intercept; S: slope.

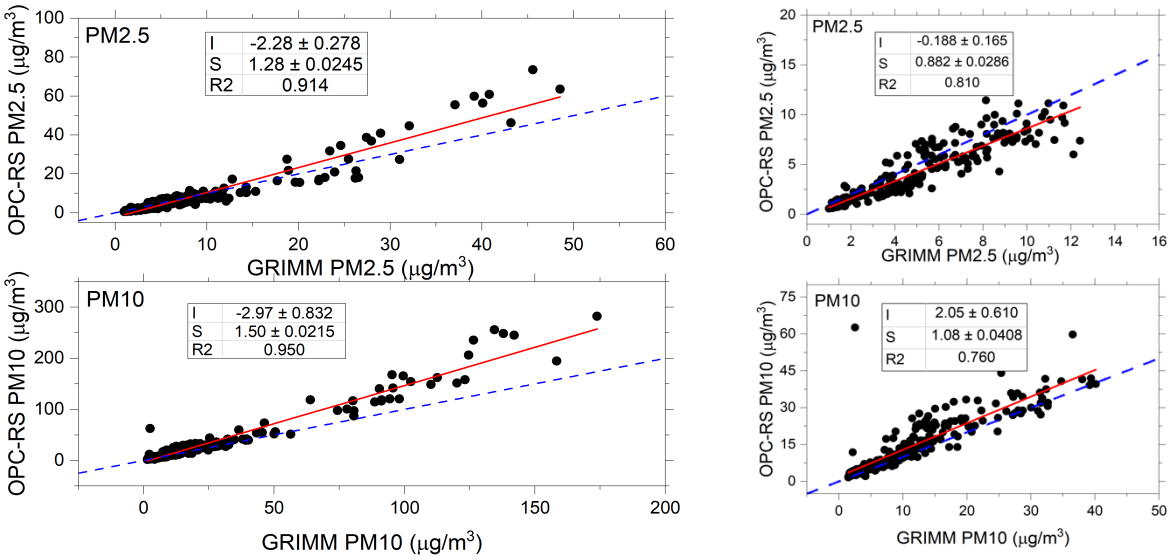

Figure S5: $PM_{2.5}$ and PM_{10} comparison for OPC-RS and GRIMM at RS site (left) using all the measurements between 04/18/2022 – 04/30/2022; (right) removing high concentrations values (PM_{10}>50 µg/m^3) to focus on typical ambient measurements. I: intercept; S: slope.

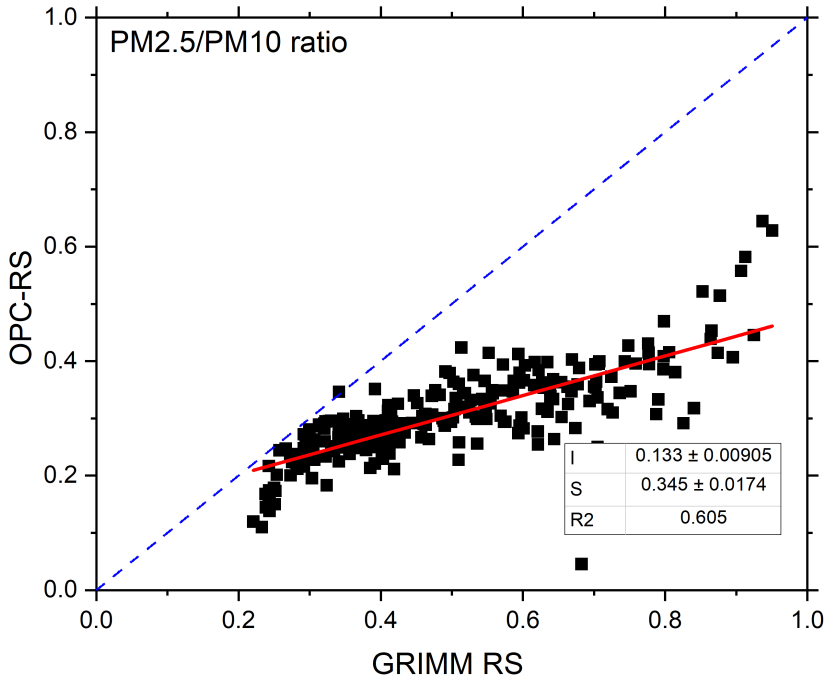

Figure S6: $PM_{2.5}/PM_{10}$ ratio for OPC-RS vs. the $PM_{2.5}/PM_{10}$ ratio GRIMM-RS. The plot includes measurements recorded between 04/18/2022 – 04/30/2022.

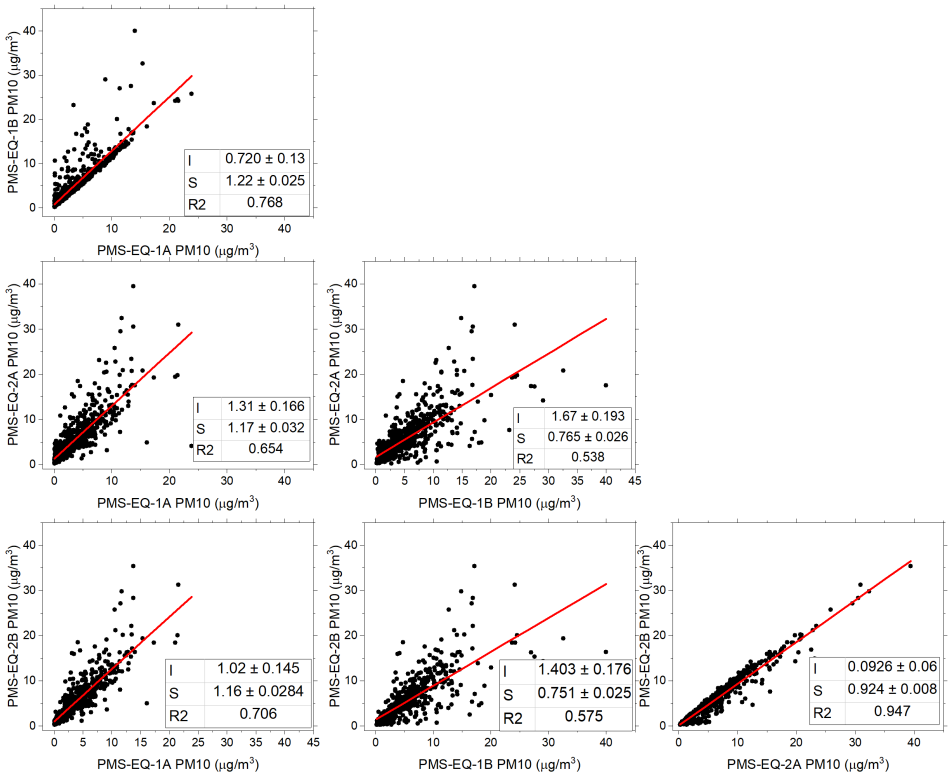

Figure S7: Inter-sensor correlation for the PMS5003 sensors at EQ. The plot includes measurements recorded between 04/1/2022 – 04/30/2022.

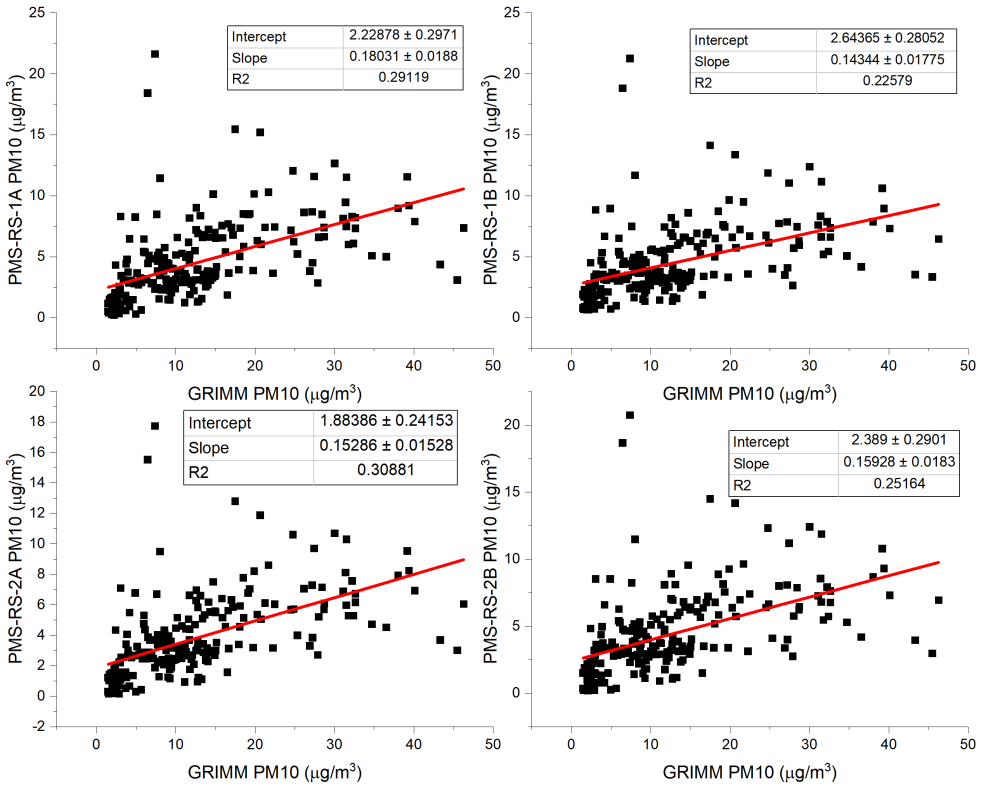

Figure S8: PM_{10} concentrations for $PM_{10} < 50$ µg/m³: Uncorrected PMS sensors vs. GRIMM at RS site.

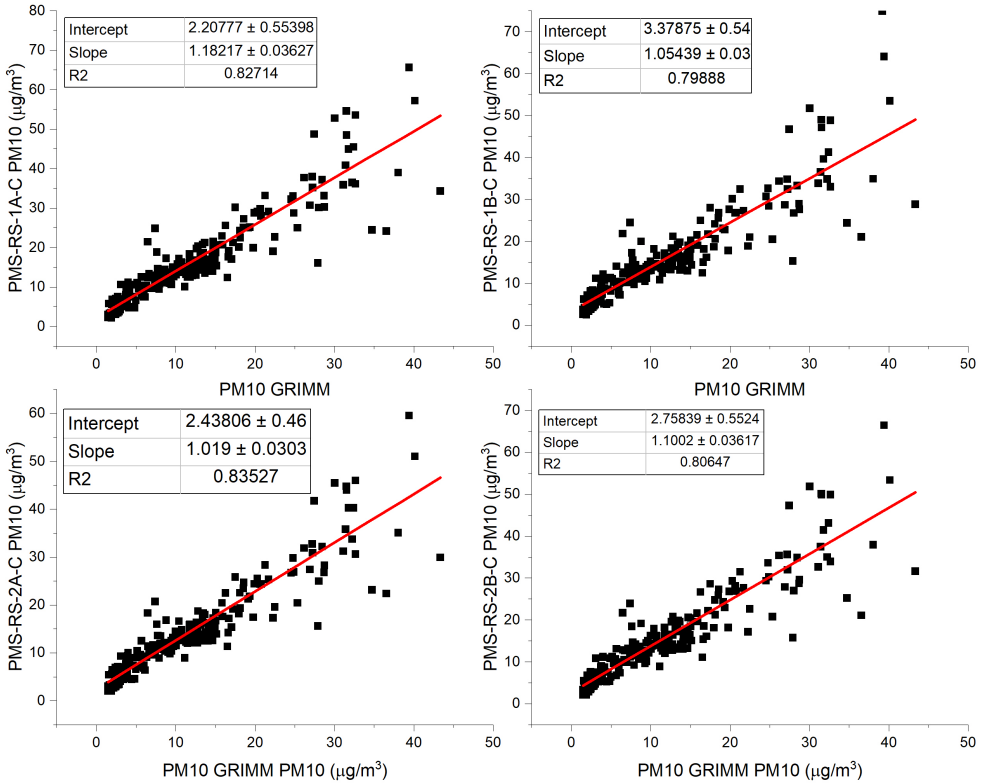

Figure S9: PM_{10} concentrations for $PM_{10} < 50$ µg/m^3 at RS. Corrected PMS sensors using GRIMM PM ratio vs GRIMM at RS site.

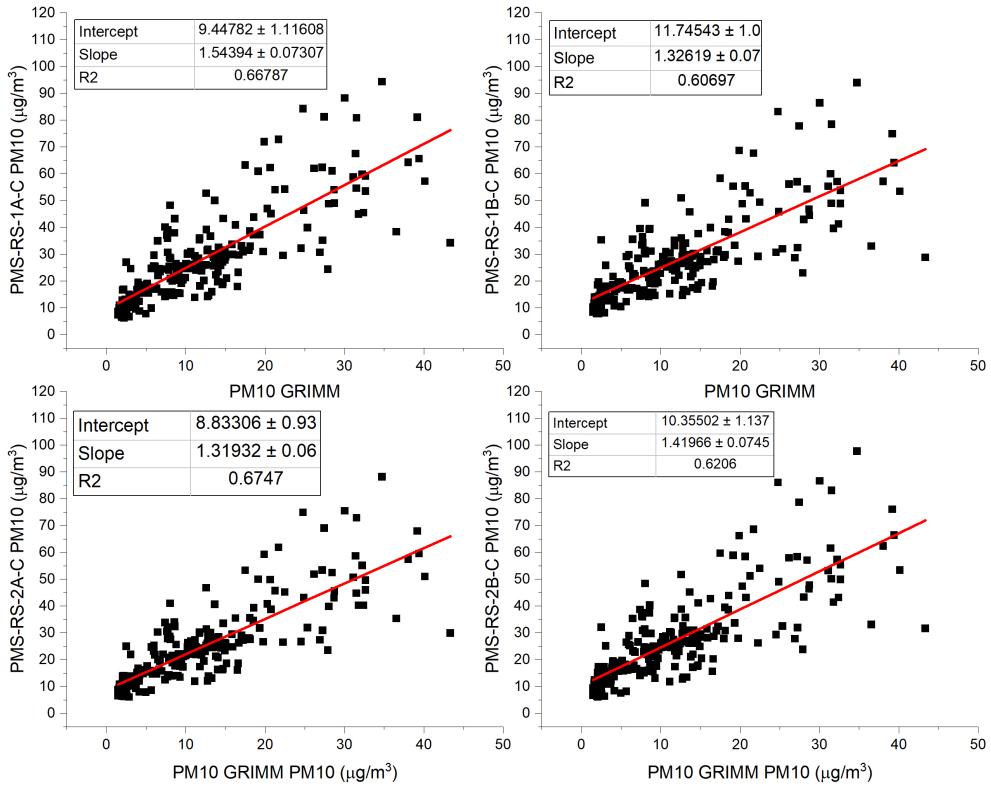

Figure S10: PM_{10} concentrations for $PM_{10} < 50$ µg/m³: Corrected PMS sensors using OPC-RS PM ratio vs. GRIMM at RS site.

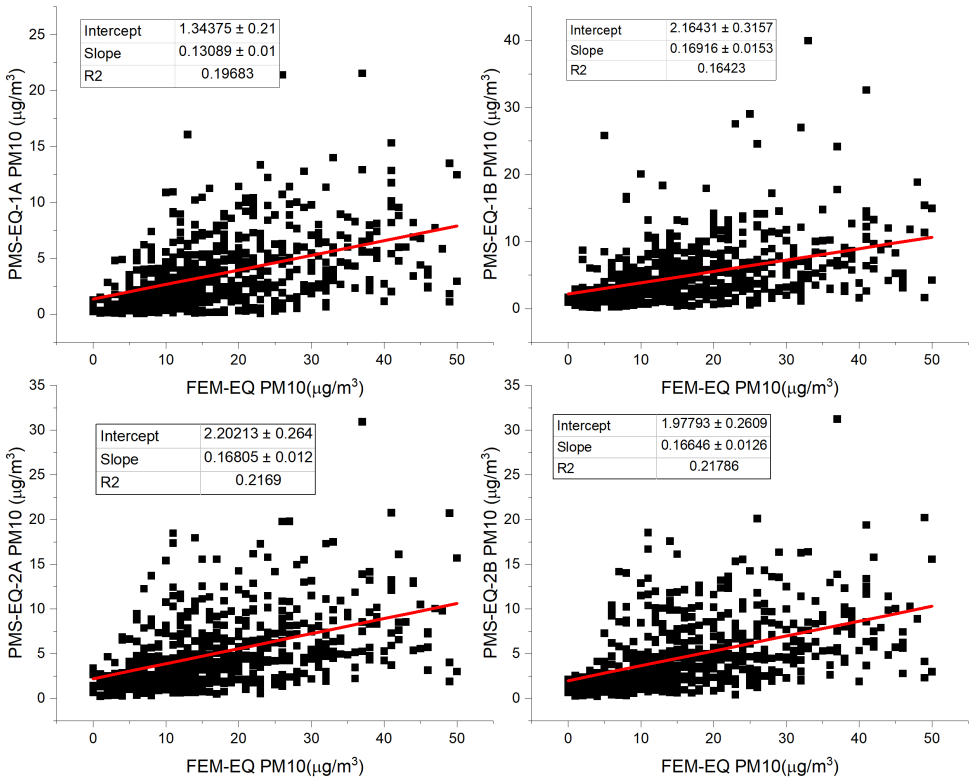

Figure S11: PM_{10} concentrations for $PM_{10} < 50$ µg/m^3: Uncorrected PMS sensors vs FEM-EQ PM_{10}.

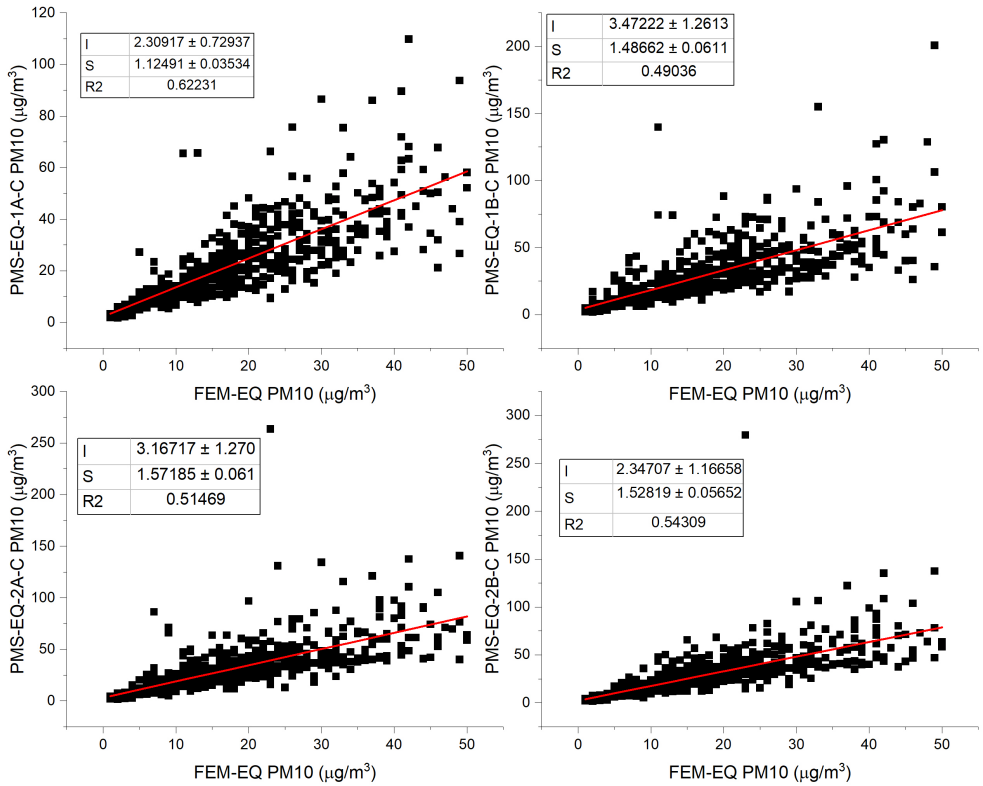

Figure S12: PM_{10} concentrations for $PM_{10} < 50$ µg/m³: Corrected PMS sensors vs FEM-EQ PM_{10}.

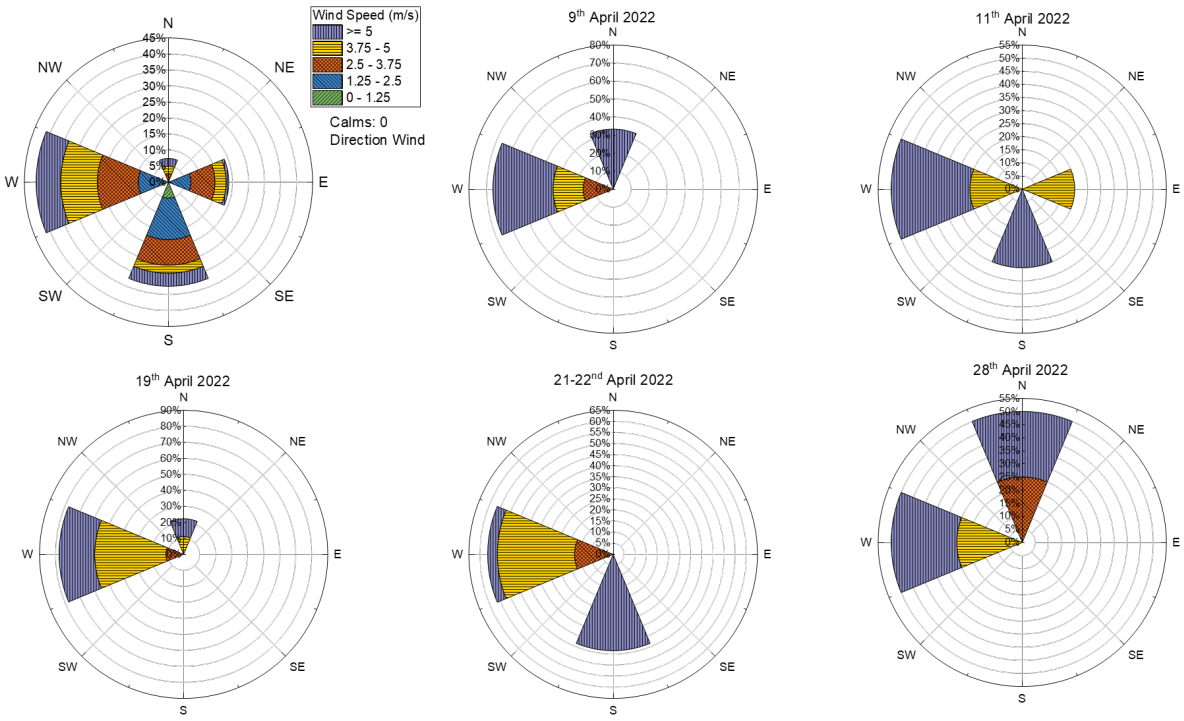

Figure S13: Wind roses at EQ monitoring station for April 2022 and individual dust events.

Table S1: Meteorological and PM characteristics during the dust events at the EQ monitoring site. The number in the parenthesis represents the minimum and maximum of the parameter.

Start	Duration (hrs)	Wind Speed (m/s)	Relative humidity %	Temperature (°C)	$PM_{2.5}/PM_{10}$	PM_{10} ($\mu g/m^3$)
4/9/22 5:00 AM	6	4.97 [3.23, 6.27]	40 [24,47]	10.2 [7.8,16.1]	0.12 [0.083,0.187]	83.3 [40,133]
4/11/22 9:00 AM	10	5.96 [3.75,8.79]	23.5 [13,43]	11.3 [6.1,15]	0.1 [0.04,0.173]	119.3 [49,302]
4/19/22 9:00 AM	9	5.51 [2.57,9.1]	25.4 [18,33]	16.2 [13.9,17.8]	0.24 [0.105,0.42]	101.33 [50,152]
4/21/22 9:00 AM	23	5.82 [2.88,9.67]	35.22 [11,69]	15.9 [7.2,23.9]	0.14 [0.059,0.25]	163.1 [45,327]
4/28/22 9:00 PM	4	5.96 [2.93, 9.61]	41.3 [32,49]	14 [11.1,17.2]	0.15 [0.046,0.254]	138.75 [37,239]

Section S2: Correcting OPC-N3 data at HW using the correlation between the OPC-N3 and the FEM-HW

Using the linear correlation obtained from the OPC-HW vs. FEM-HW (Figure S14 left), the OPC-N3 data was corrected to check for any improvement in the RMSE. The RMSE increased slightly to 12.9 from 12.4 µg/m^3 after correction. The slope improved from 0.92 to 0.99, but the R^2 remained constant.

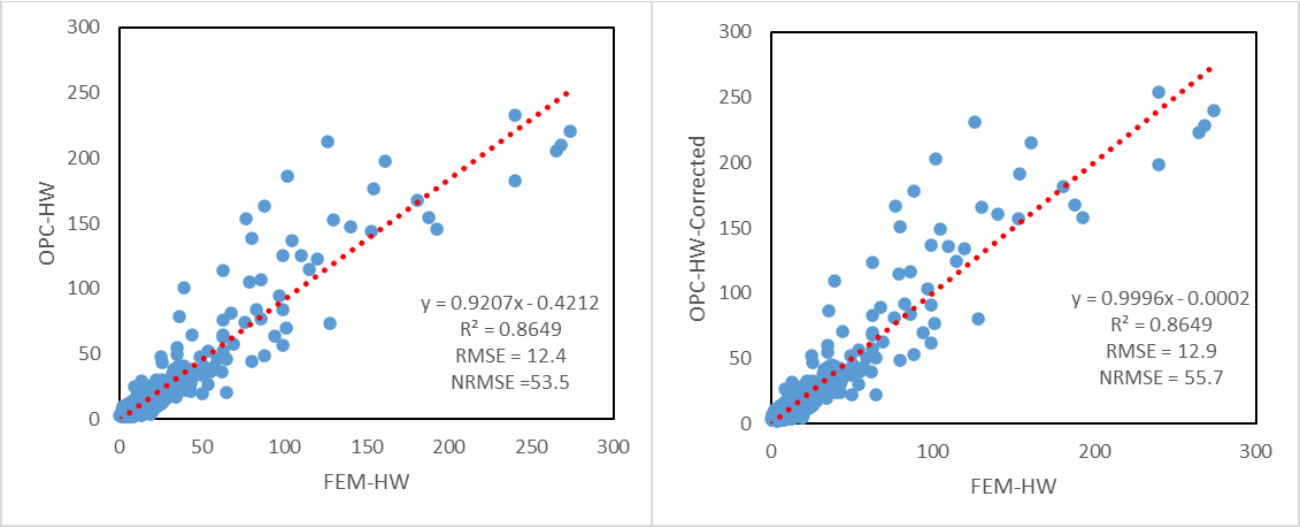

Figure S14: OPC-N3 vs BAM at HW: (left) OPC-HW vs FEM-HW; (right) Corrected OPC-HW vs FEM-HW.

Section S3: Housing for the OPC-N3

A custom housing was built for OPC-N3 to protect the sensor from rain (Fig.S15). The housing includes: 1) opening for sensor inlet; 2) a small hood to protect from rain; 3) opening for air circulation; 4) opening for the wiring. The sensor bottom has drainage port (not visible in the Fig. S15), in case water entered from the opening at the back of the housing.

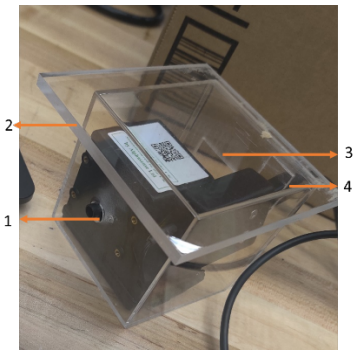

Figure S15: Housing for the OPC-N3. The number 1, 2, 3, and 4 represent opening for the inlet, hood for the sensor, opening for air circulation, and opening for the wiring, respectively.